

Electromagnetic Simulation of Non-Invasive Approach for the Diagnosis of Diabetic Foot Ulcers

Roshen Borkar¹, James Rizkalla², Youngmin Kwon¹, Paul Salama¹, and Maher Rizkalla^{1,3}

1. Department of Electrical and Computer Engineering, IUPUI
2. Baylor University Medical Center, Dallas, Texas
3. Integrated Nanosystems Development Institute, IUPUI

Abstract

Diabetic foot ulcers are systemic diseases that affect all blood vessels within the human body. From major blood vessels to microvasculature, hardening, thickening, and narrowing of blood vessels ultimately results to diminished blood flow to end organs. The detrimental effects of peripheral vascular disease are well recognized across medicine, particularly with regards to diabetic foot ulcers. Diabetic foot ulcers (DFU) are common across all fields of medicine, including but not limited to: orthopedics, vascular surgery, podiatry, general internal medicine, and infectious disease. As the population of the United States continues to grow in age and obesity, diabetes and DFU are becoming more and more prevalent in our medical society. Current approaches to diagnosing peripheral vascular disease ultimately result in some degree of invasiveness for the patient. Preliminary lab studies, such as the ankle-brachial index and Doppler ultrasound of peripheral arteries, provide efficient safe screening methods. However, these studies lack quantification of the degree of vascular stenosis and are unable to accurately assess the location of narrowing. In current practice, radiologists are called upon to for angiography of the blood vessels using contrast dye. This provides an additional risk for diabetic patients: a population inherently at risk for renal disease.

In this study, we proposed utilizing electromagnetic simulation with boundary conditions set at various layers of human tissues. More specifically, the human foot was analyzed using COMSOL multi-physics software in attempt to visualize, analyze, and quantify the degree of peripheral vascular disease, which plays a pivotal role in the development of diabetic foot ulcers. The simulation was conducted for a patient's foot, with bone, blood vessels, and surrounding fat layers to emulate the anatomy of a diabetic foot. A 2-D scan was obtained to assess and visualize the blood vessel's narrowing, widening, vascular turbulence, or occlusion. The analysis was conducted at two frequencies, 2GHz and 5GHz, and compared to one another to assess the accuracy of clinical diagnosis. An electric field was generated throughout the 2D model at 20, 50, and 100 Joules, respectively. The simulation was able to adequately predict and stratify varying degrees of occlusion within peripheral vasculature. This study, though a simulation in nature, shows promise for being able to accurately diagnose the peripheral vasculature using electromagnetic parameters. This feasibility study proved successful for possible future implementation using MEMS/NEMS device systems to be designed to detect EM parameters to serve as a diagnostic tool for the early detection of peripheral vascular disease, and ultimately, diabetic foot ulcers.

This is the author's manuscript of the article published in final edited form as:

Borkar, R., Rizkalla, J., Kwon, Y., Salama, P., & Rizkalla, M. (2018). Electromagnetic simulation of non-invasive approach for the diagnosis of diabetic foot ulcers. *Journal of Orthopaedics*, 15(2), 514–521. <https://doi.org/10.1016/j.jor.2018.03.024>

Key words: Ortho; COMSOL; Diagnosis; non-invasive; blood vessel blockages

I. Introduction

Human Arterial system is a blood circulation feeding various body members, and may be affected by narrowing, widening, or blocking the blood path at any section in the arterial system [1]. The blocking of the artery may be attributed to cholesterol deposits within the vein's boundary. This is known as atherosclerosis (the narrowing of veins) [1]. This may result in painful or numbness foot, and may lead to ischemia of the foot [2]. This may be seen often in diabetics and orthopedic patients [3]. In normal patients, this may occur when there is no adequate blood flow, leading to sore development [4], which is frequently managed by orthopedic surgeons. In orthopedic, patients may suffer from muscle weakness and/or brittle bone. Varicose veins (Large cross-sectional area) may cause inability to maintain a regular blood flow within the blood circulation of the human system [5]. Less resistive flow in large veins/ varicose veins may imbalance affecting the blood flow from the source (heart). Varicose veins may cause chronic swelling in the foot, and ankles among others [6]. A serious issue that may occur from the vein narrowing is the blood clots that may lead to some pulmonary disease which could be life threatening to the patients [7].

The impact of the blood vessels widening and narrowing can be easily understood from the circuit model such as the one shown in figure 1 [8]. If a vein is narrowed within the blood circulation, this is equivalent to a higher resistance that may affect the blood flow near the artery (the source). Likewise, if a vein is widened, this will be equivalent to a reduction in the resistance for the blood flow, leading to a higher blood flow drawn from the source. In either case, this may affect the output performance of the human heart.

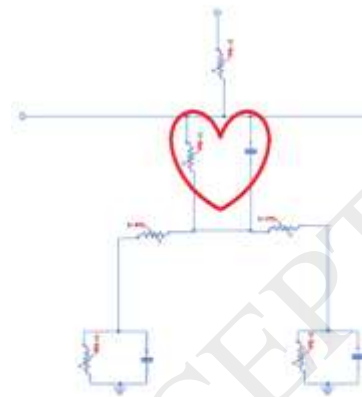


Figure 1: The circuit model of blood circulation within the human body.

Treatment of vein problems may need general surgery or invasive approach such as vascular surgery or inferential cardiovascular surgery. Medications are currently used in order to reduce the effect of blood vessels narrowing but may temporarily be reducing pain or dissolving clots. Medical imaging has been used for the investigation of vein narrowing in order to address the seriousness of the disease. Among those are ultrasound or ultrasonography [9] in identifying symptoms and causing signs of blood narrowing or artery narrowing [10]. However, the Sonographic Elasticity imaging (SEI) is a noninvasive approach, it cannot assist the maturity of the case and cannot detect the chronic clots [11]. CT and MRI are commonly used as tools to visualize the central veins or test the presence of complications in

Pulmonary Diseases [12]. The cost and accuracy involved in this tool sets limit to their application within the human foot.

In this study, we propose electric field scanning on the surface area of the foot skin, ankle, or others to detect the narrowing, widening, and blocking within veins via the blood circulation system. The simulation done here was by applying two high energy levels (10J and 100J energy) at 3 and 5 GHz values. The transmission properties of the electric field distribution between layers, and among the veins, bones, and skin, lead to the determination of the field parameters.

II. The EM Models

The wave equation used in the determination of the E distribution is given below:

$$\nabla \times (\nabla \times E) = \nabla (\nabla \cdot E) - \nabla^2 E$$

From Gauss 'law, $\nabla \cdot D = P_v$, then $\nabla \cdot E = P_v/\epsilon$

Using $P_v = 0$, the wave equation becomes:

$$\nabla \times (\nabla \times E) = -\nabla^2 E$$

The electric field is given in the form:

$$E = E_0 e^{-\gamma z}$$

where γ = Propagation constant determined from:

$$\gamma^2 = -\omega^2 \mu \hat{\epsilon}$$

where $\hat{\epsilon}$ is the complex permittivity given as:

$$\hat{\epsilon} = \epsilon(1 - j\sigma/\omega\epsilon)$$

when $\epsilon = \epsilon_0 \epsilon_r$

$$\omega = 2\pi f$$

σ = conductivity

The propagation constant, γ , is given by:

$$\gamma = \alpha + j\beta$$

Where α is the attenuation constant, and β is the Phase shift constant. The electric field is then given by:

$$E = E_0 e^{-\alpha z} e^{-j\beta z}$$

The magnitude of the field is given by:

$$E = E_0 e^{-\alpha z}$$

The boundary conditions used in this analysis were based on matching the tangential components of the electric fields at the interfaces, fat/vein/bone boundaries. That is $n \times E = 0$ at the interfaces.

III. Results and Discussions

The research conducted here covers data for normal patients “all veins have the same size” as well as patients with vein issues disease (such as narrowing, widening, and missing). The study considers a foot size of 10 cm x 20 cm x 1 cm about 160 steps were generated from the software to track the electric field changes across the fat, bone, and vein materials. Initially 3GHz signals simulation can be used to detect the presence of the veins. Based on the results of 3GHz signal results we can implement 5Ghz signal simulation to measure the thickness of the veins. Table 1 gives the material properties used in the simulation

Table 1: Material properties used in the simulation

Material	Frequency	Relative Permittivity	Conductivity (mho/m)
Bone	2 GHz	4.9	0.15
	5 GHz	0.8	0.21
Muscle	2 GHz	55.4	1.45
	5 GHz	49.6	2.56
Fat	2 GHz	15	0.35
	5 GHz	12	0.82

3.1 The Mesh Graph

Figure 2 shows the computer mesh model used in the simulation with finer mesh of 0.5mm to 1mm. This mesh was used to get better accuracy of the field distribution output.

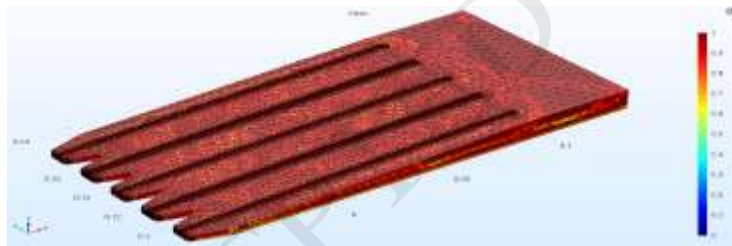


Figure 2: Mesh figure

3.2 Vein Detection for Normal Patients

COMSOL simulation was conducted to detect normal patient condition with all veins having the same size. The veins were surrounded by fat materials. The electric field distribution across the fat showed maximum value, while inside the vein was minimum. The size of the veins was easy to detect since they are surrounded by fat materials from both sides. In this study also, we considered two different frequencies, 3 GHz and 5 GHz for the investigation of the E-field distribution over the human foot, with energy levels ranges between 20 and 100 joules. A threshold field was set based on simulation results, and the thicknesses of the veins were estimated. Figures 3 to 6 show the E distribution for five veins surrounded by fat materials. Figure 3 gives the distribution at 3 GHz for 20-joule pulse energy. The 5 GHz field distributions are given in figure 4. It is clear that the 3 GHz data did not accurately designate the depth of the vein sizes, while 5 GHz data showed consistent results for the vein sizes. Out of the

three energy levels used in the study, 5 GHz with 100 Joules produced better accuracy with field distribution way higher than the threshold values. The size of the veins was determined from the distance between the two fat materials. Figures 5 and 6 give the distribution for 3 GHz and 5 GHz given at 50-Joule pulse energy. The 100-joule energy pulse with at 3 GHz and 5 GHz are given in figures 7 and 8 respectively. Figure 9 gives the digital distribution for the field data, generated in order to estimate the artery sizes based on the threshold values. This data was generated based on setting logic high for vein size, with zero for the fat materials. In this case, the size of the veins can be easily detected. The digital format of the E-distribution may easily assist with characterizing the patient disease.

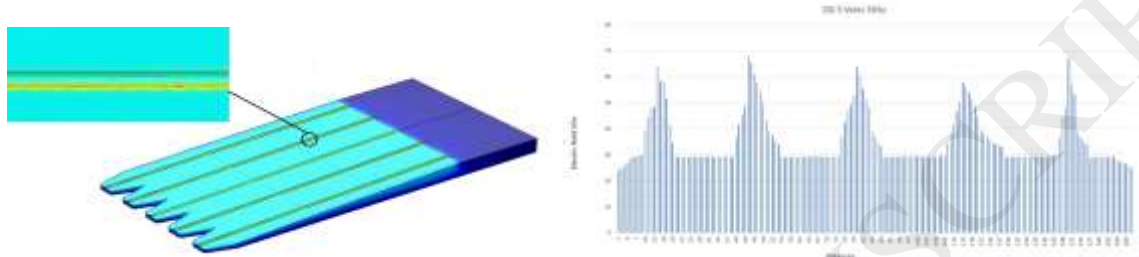


Figure 3: E-distribution for 20 Joules 5 Veins 3 GHz

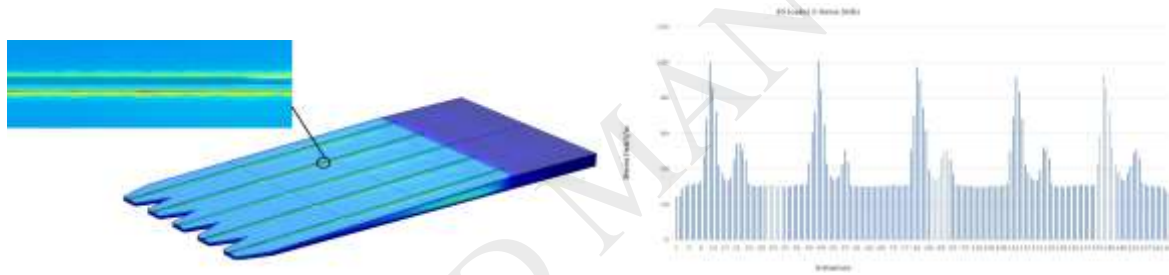


Figure 4: E-distribution for 20 Joules 5 Veins 5 GHz

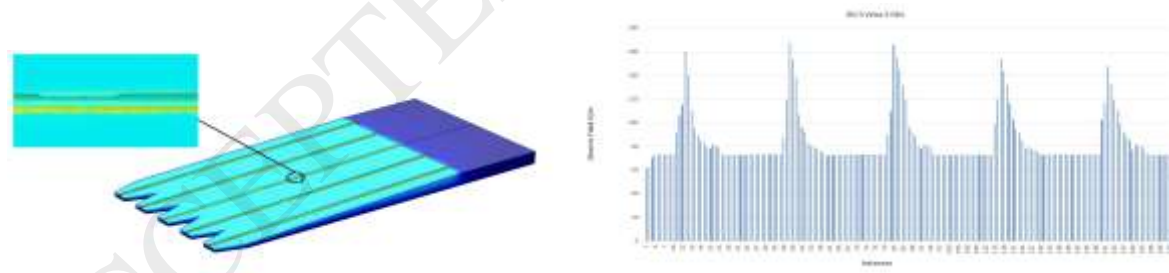


Figure 5: E-distribution for 50 Joules 5 Veins 3 GHz

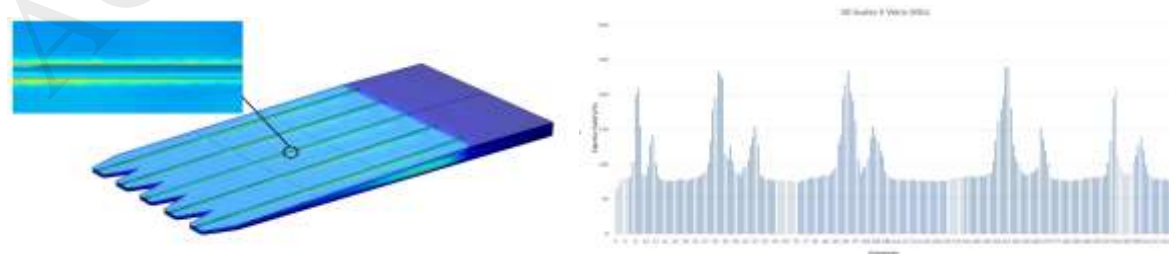


Figure 6: E-distribution for 50 Joules 5 Veins 5 GHz

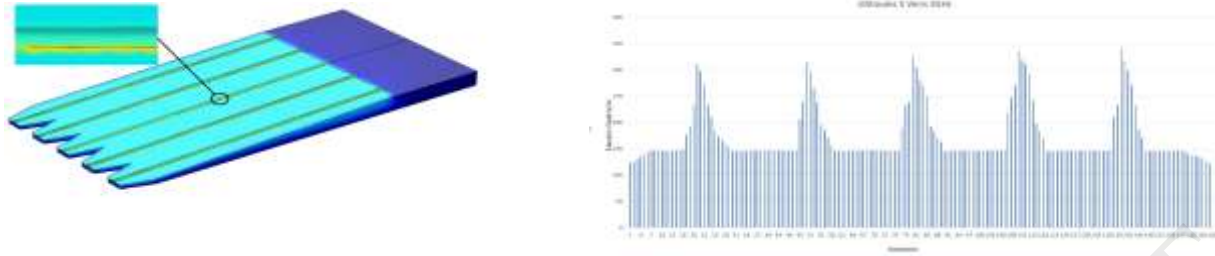


Figure 7: E-distribution for 100 Joules 5 Veins 3 GHz

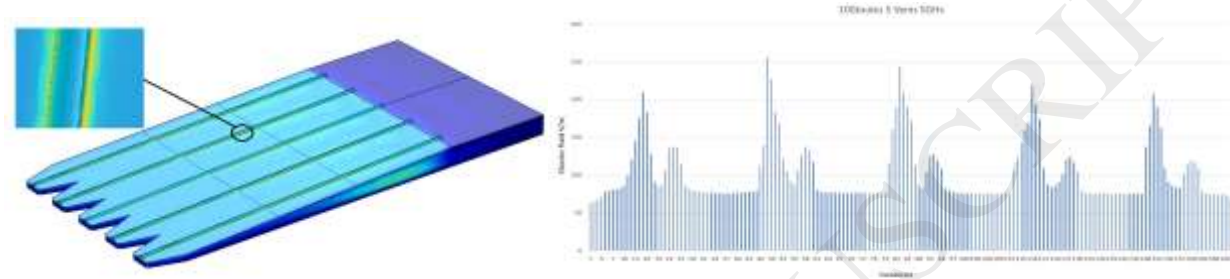


Figure 8: E-Distribution for 100 Joules 5 Veins 5 GHz

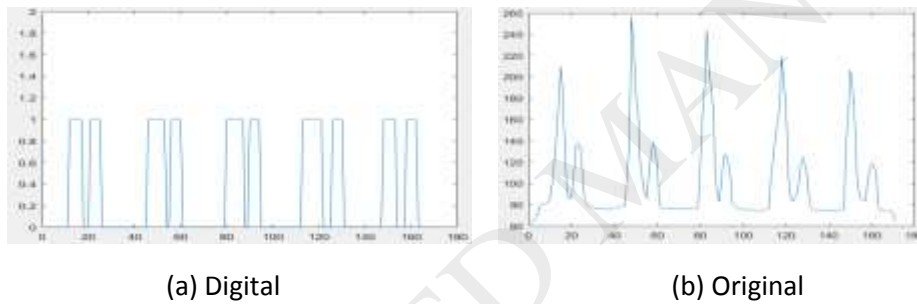


Figure 9: Digital Distribution

3.3 Narrowing and Missing Veins (for arteriosclerosis disease)

Figures 10 to 15 give the field distribution for narrowing and missing vein materials. Figure 13 show the digital format of the field distribution, indicating the vein sizes. In this case, for instance, vein number 1, 3 and 5 are narrower than 2 and 4 vein. In figure 10, veins 1, 2 and 4 was missing based on the field distribution.

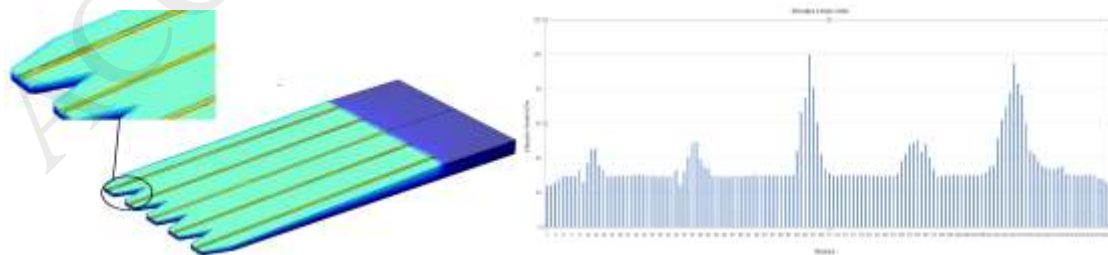


Figure 10: E-Distribution for 20 Joules 2 Veins 3 GHz

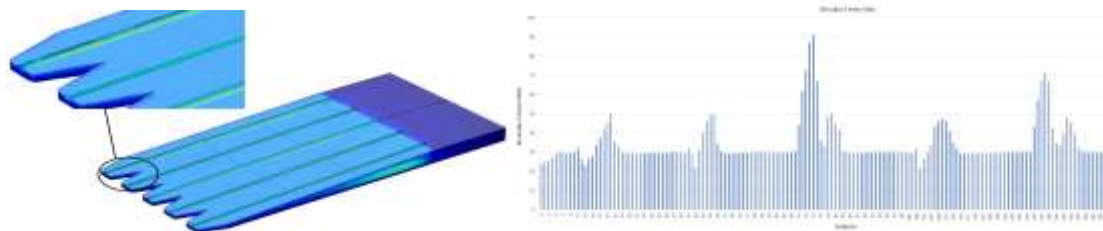


Figure 11: E-Distribution for 20 Joules 2 Veins 5 GHz

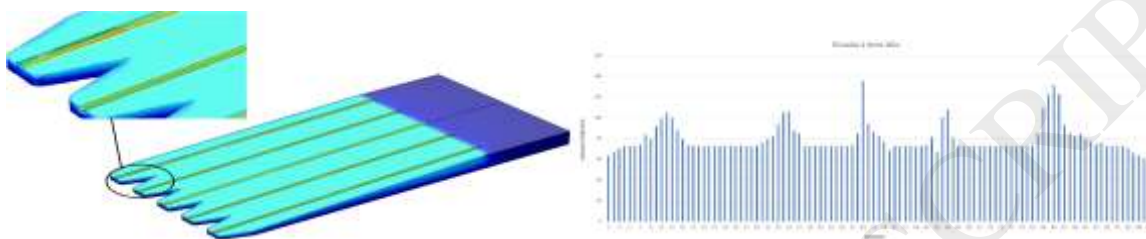


Figure 12: E-Distribution for 50 Joules 2 Veins 3 GHz

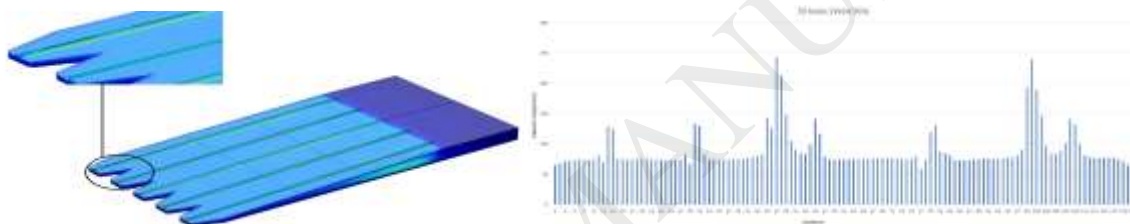


Figure 13: E-Distribution for 50 Joules 2 Veins 5 GHz

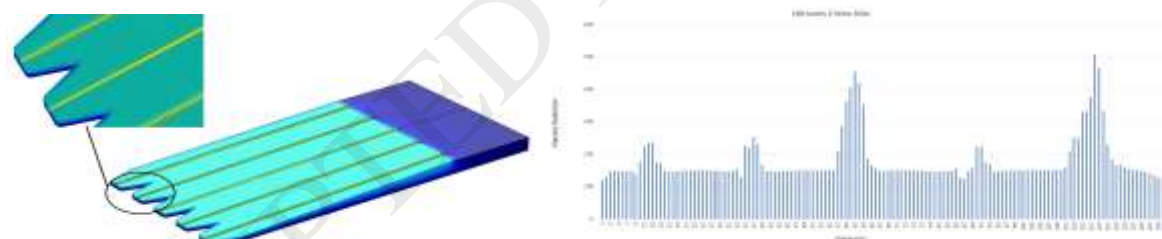


Figure 14: E-Distribution for 100 Joules 2 Veins 3 GHz

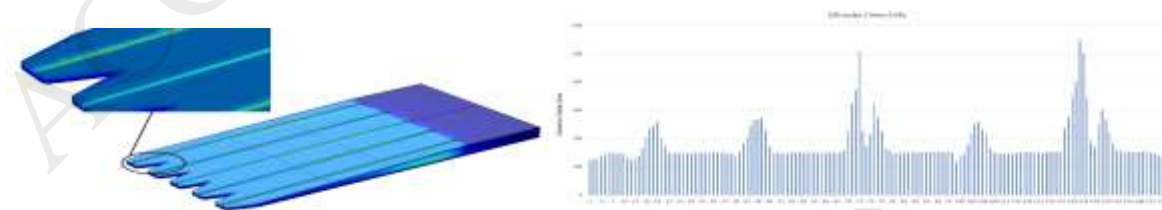


Figure 15: E-Distribution for 100 Joules 2 Veins 5 GHz

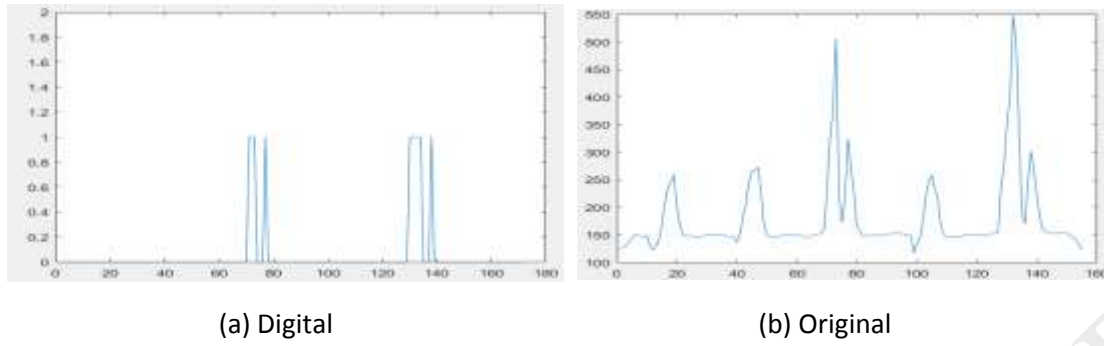


Figure 16: Digital-Distribution for missing vein

3.4 Widening Veins Vasodilation

The widening data was also studied. Figures 17 to 22 cover the same information as above with respect to the widening of the veins. Figure 18 gives the digital format of the distribution with clear vein widening.

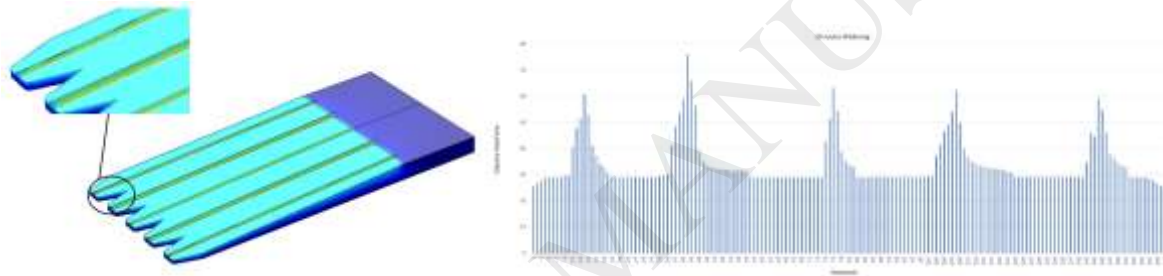


Figure 17: E-Distribution for 20 Joules 2 Veins 3 GHz Widening

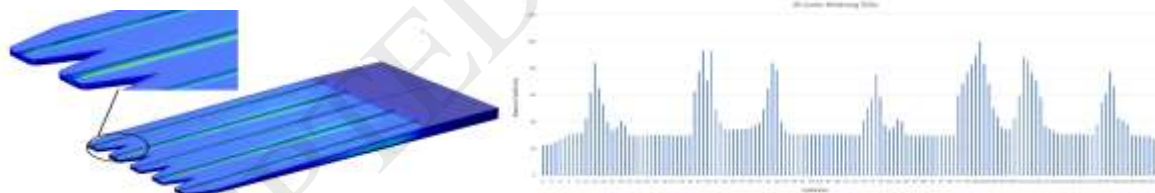


Figure 18: E-Distribution for 20 Joules 2 Veins 5 GHz Widening

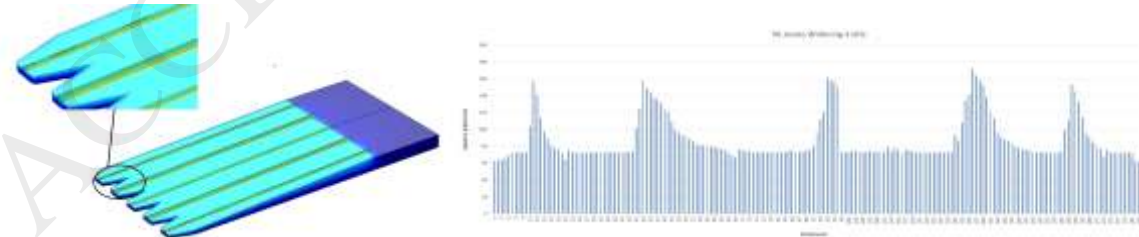


Figure 19: E-Distribution for 50 Joules 2 Veins 3 GHz Widening

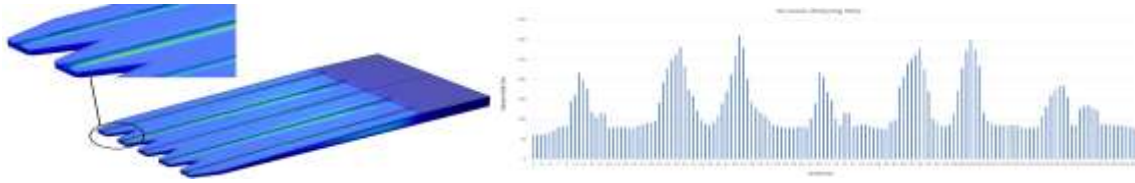


Figure 20: E-Distribution for 50 Joules 2 Veins 5 GHz Widening

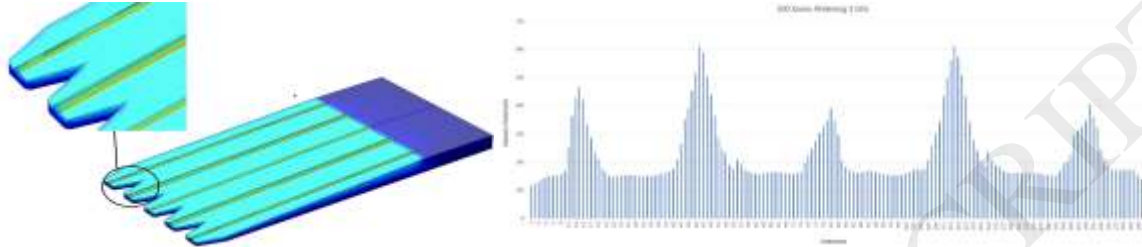


Figure 21: E-Distribution for 100 Joules 2 Veins 3 GHz Widening

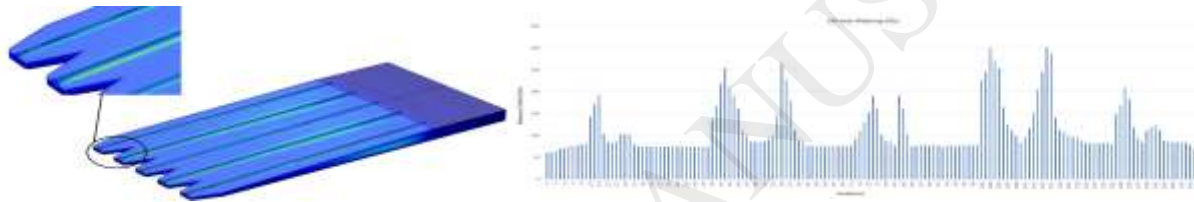


Figure 22: E-Distribution for 100 Joules 2 Veins 5 GHz Widening

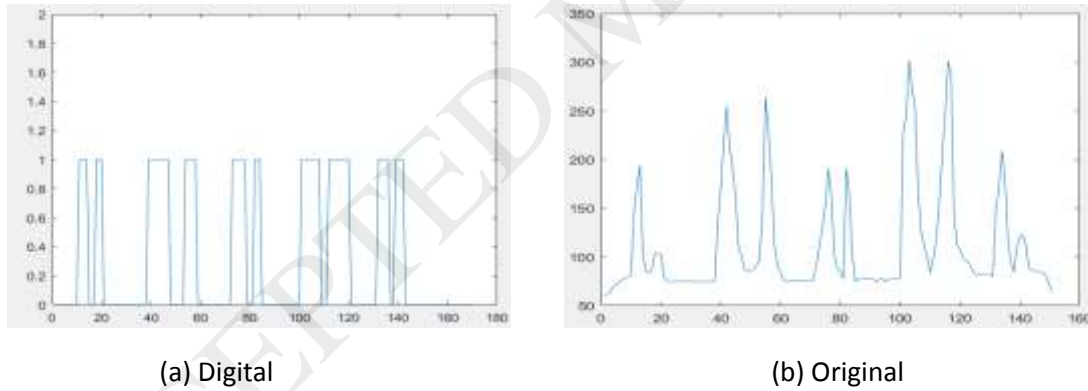


Figure 23: Widening Digital Distribution

Results and Discussions:

In this simulation the frequency, power and vein sizes were the parameters under investigation. Two values of frequency was considered 3GHz & 5GHz, and 3 different power values; 20, 50, and 100 joules. The vein sizes were categorized between widening, narrowing and blocking. The output resulting from these parameters was an electric field quantity. As it is clear in figures 1 to 12 the 5GHz frequency indicated higher quality imaging showing the electric field as reflected by the size of the veins. In this practical implementation the sensor devices in 2D array detecting the values of electric field translated into voltage values and fed into a sample and hold off circuit. The output waveform of this circuit will be in a digital format where the logic high indicates the high density electric field with a width of the vein

figures 19 onwards show the width of the veins within the 3 categories widening, narrowing and blocking. Some of these outputs show the missing veins indicating by the reduction of electric field within that distance. Figures 1 to 6 show the output waveform for 3 GHz. 7 to 18 show the effect of the power change. in our analysis a threshold value for electric field translated from hall effect devices translating them into voltages and were given data to the sample and hold off circuit. Table 1 summarizes the impact of the frequency power and sizes within the output voltage given within a range. The 5GHz data shows better imaging/ clear signal, and this is attributed to the proper values of the permittivity and electric conductivity at this particular frequency as compared to 3 GHz. The power values 20 and 50 were chosen in order to produce proper electric field values that are appropriate to be measured by the existing Hall effect devices for future implementation of the system

Conclusion and Future work

The study conducted here was a proof of concept for non-invasive diagnosis of using EM power transmission. The data suggested 100 joule pulse energy with comparative field data at 3 GHz and 5 GHz. In the practical future model, 2-D sensors should be built to detect the field data from a sample and hold off circuit as shown in figure 25. The digital data form may be obtained from a comparator circuit such as the one suggested in figure 24.

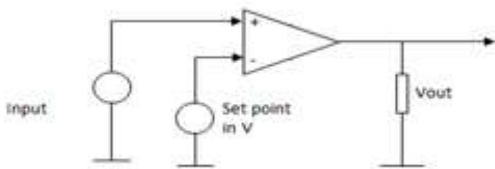


Figure 24: Circuit for Digitization

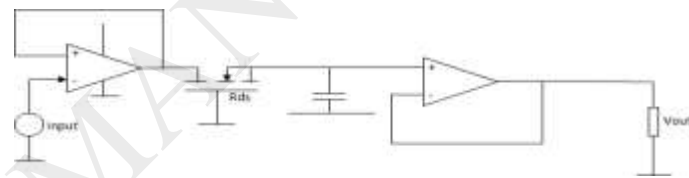


Figure 25: Sample and Hold Circuit

Acknowledgement

The authors would like to acknowledge the assistance of INDI staff and faculty for their assistance with using COMSOL during this research. The authors also would like to offer their appreciation to Mr. Rajat Sharma, a graduate mechanical engineering student at IUPUI for his assistance with the model used in this research.

Author's contributions

Both Mr. Roshen Boker and Mr. Youngmin Kwon are graduate engineering students working on the simulation of the foot using COMSOL multi Physics. Both are conducting the EM simulation of the foot ulcers. Roshen is an expert in EM simulation, while Kwon does the study at the system level. Dr. James Rizkalla introduced the medical issue that was extracted from his clinical and research work at Baylor University Medical center. Dr. Maher Rizkalla is the advisor for both Roshen and Kwon. Dr. Salam's expertise is in medical imaging. He conducts the comparative study for better approach compared to the existing technology.

References:

1. <https://www.webmd.com/heart-disease/atherosclerosis-and-coronary-artery-disease#1>
2. Wikipedia, <https://en.wikipedia.org/wiki/Vasodilation>
3. Schaper NC, Van Netten JJ, Apelqvist J, et al. Prevention and Management of Foot Problems in Diabetes: A Summary Guidance for Daily Practice Based on the 2015 IWGDF Guidance Documents". Diab Metab Res Rev. DOI: 10.1002/dmrr.2695
4. Kerr M, Rayman G, Jeffcoate WJ. Cost of diabetic foot disease to the National Health Service in England. Diabet Med 2014; 31(12): 1498–504.
5. Evans CJ, Fowkes FGR, Ruckley CV, Lee AJ. Prevalence of varicose veins and chronic venous insufficiency in men and women in the general population: Edinburgh Vein Study. J Epidemiol Community Health 1999;53:149-53.
6. Veldman PH, Reynen HM, Arntz IE, Goris RJA. Signs and symptoms of reflex sympathetic dystrophy: prospective study of 829 patients. Lancet 1993;342:1012-6.
7. Latson LA, Prieto LR. Congenital and acquired pulmonary vein stenosis. Circulation. 2007;115:103–108.
8. Ayyub BM, Koko TS, Blair A, Akpan UO. Risk Assessment Methodology for Electric-Current Induced Drowning Accidents. ASME. ASME J. Risk Uncertainty Part B. 2016;2(3):031004-031004-14. doi:10.1115/1.4032308.
9. Elias A, Le Corff G, Bouvier JL, Benichou M, Serradimigni A. Value of real time B mode ultrasound imaging in the diagnosis of deep vein thrombosis of the lower limbs. Int Angiol 1987; 6 (2): 175-82.
10. Rubin, J. M., Xie, H., Kim, K., Weitzel, W. F., Emelianov, S. Y., Aglyamov, S. R., Wakefield, T. W., Urquhart, A. G. and O'Donnell, M. (2006), Sonographic Elasticity Imaging of Acute and Chronic Deep Venous Thrombosis in Humans. Journal of Ultrasound in Medicine, 25: 1179–1186. doi:10.7863/jum.2006.25.9.1179
11. Hoffman EA, Lynch DA, Barr RG, van Beek EJR, Parraga G. Pulmonary CT and MRI Phenotypes that help explain COPD Pathophysiology and Outcomes. *Journal of magnetic resonance imaging : JMRI*. 2016;43(3):544-557. doi:10.1002/jmri.25010.